Article

Not peer-reviewed version

Soil Mercury Pollution of the Hainan Island, China: Pattern, Influencing factors and Health Risk

Yan Sun and Canchao Yang *

Posted Date: 26 February 2024

doi: 10.20944/preprints202402.1449.v1

Keywords: Hainan Island; soil mercury; pollution characteristics; health risk assessment

Article

Soil Mercury Pollution of the Hainan Island, China: Pattern, Influencing Factors and Health Risk

Yan Sun [1,2] and Canchao Yang [1,2,*]

[1] College of Life Sciences, Hainan Normal University, Haikou 571158, China; isotope2014@163.com (Y.S.)
[2] Ministry of Education Key Laboratory for Ecology of Tropical Islands, College of Life Sciences, Hainan Normal University, Haikou 571158, China; kingfisher.ycc@163.com (C.Y.)
* Correspondence: kingfisher.ycc@163.com

Abstract: Due to the growth of tourism, mining and manufacturing, economy of the Hainan Island, southern China has swiftly expanded, but also poses a risk of soil pollution by mercury (Hg) due to the traffic and mineral processing. In order to investigate the characteristics of soil Hg pollution in the Hainan Island and assess the health risk, a total of 239 samples were gathered from five representative regions across the island. A vehicle-mounted potable mercury analyzer was used to measure the atmospheric Hg and soil Hg concentrations in the collected samples. The results indicate that the soil Hg concentration of the five sub-study areas exhibits notable fluctuations, which was found to be influenced by various factors, including wind direction, mining activities, and economic development conditions. The degree of Hg pollution was assessed using both the Single Pollution Index Method and the Geoaccumulation Index Method. The results showed that although nearly half of the sampling points were contaminated, the current soil Hg level does not pose a non-carcinogenic risk to human health.

Keywords: Hainan Island; soil mercury; pollution characteristics; health risk assessment

1. Introduction

Mercury (Hg) is a highly toxic pollutant (Meriga, 2004; Futsaeter, 2013; Carocci, 2014). The Minamata Disease, which took place in 1956, Japan, stands as the most famous environmental hazard incident resulted from Hg pollution (Cheng, 2008). Since then, numerous incidents of Hg pollution have been documented globally (Taylor, 2000; Martin et al., 2004), prompting increased attention to Hg pollution. Due to its distinctive physiochemical properties, Hg can easily amass in living organisms, posing a lethal threat to human (Hu, 2008); hence, it has been designated a global pollutant by the United Nations Environment Program. The atmosphere serves as the primary medium for Hg migration in nature. Gaseous Hg (GEM) is prevalent in the atmosphere with a low dry deposition rate, high solubility in water, and relatively prolonged residence time of 0.5 to 1.5 years, facilitating its long-range transport through the atmosphere (Kang et al., 2018). Soil serves as a reservoir for Hg in the environment, with soil Hg pollution characterized by latency, persistence, high toxicity, and irreversibility (Yin et al., 2009), thus representing a critical aspect of the Hg pollution issue. Urban soil Hg pollution has direct effects on public health, underscoring the profound importance of comprehensively assessing the Hg pollution status of urban soil.

The main sources of Hg consist of human activities (Xu et al., 2015) and natural processes (Lindberg et al., 2007). Human activities, such as the combustion of fossil fuels, non-ferrous metal smelting, Hg product generation, and waste disposal and incineration, result in the release of Hg into the environment (Fang et al., 2004; Rodrigues et al., 2006; Zhang and Wang, 2007). Researches indicate that the annual amount of anthropogenic emissions into the atmosphere is approximately 1960 t (Friedli et al., 2003, Xu et al., 2015). Recent studies have demonstrated that anthropogenic emissions exceed natural emissions, with the majority of Hg re-emissions originating from anthropogenic sources (UNEP, 2013). As the largest coal consumer and Hg emitter in the world, coal consumption dominates China's atmospheric Hg emissions (Chen et al., 2017; Zhao et al., 2019).

 doi:10.20944/preprints202402.1449.v1

Numerous studies have been conducted in order to investigate the status of Hg pollution in the air in Chinese cities, e.g., Chongqing (Li et al., 2006), Guangzhou (Yin et al., 2009), Nanjing (Huang et al., 2007), Xuzhou (Wang et al., 2005), Guilin (Qian et al., 2000), Beijing (Zhang et al., 2006), and Taiyuan (Guo et al., 1996). Furthermore, soil Hg concentration have also been studied in central cities and regions such as Tibet (Zhang, 1994) and Urumqi (Hu, 2003) in China, Palermo, Italy (Manta et al., 2002), Glasgow, UK (Rodrigues et al., 2006), Khabarovsk, Russia (Kot and Matyushina, 2002), and Aveiro, Portugal (Rodrigues et al., 2006). The results indicate varying degrees of Hg pollution in these cities, with a positive correlation between the level of urban development and the extent of pollution (Zhou et al., 2024), mining, industry and residences which cause Hg emissions (Guo and Wang, 2023).

The Hainan Island, situated in southern China, has experienced substantial economic growth in recent years, emerging as a burgeoning urban agglomeration primarily focused on tourism and external trade. Nonetheless, this rapid economic development has engendered significant environmental challenges. This study aims to investigate the present Hg pollution status in the Hainan Island by examining five representative regions on the island, analyzing the contributing factors of Hg pollution, and assessing its associated health risks. The findings will furnish valuable insights for controlling Hg pollution.

2. Study area

The study focused on the Hainan Island as the research area and collected samples from five representative regions, including Wuzhishan Nature Reserve (B) as well as four economically developed coastal cities, i.e., Changjiang Li Autonomous County (NW), Haikou (NE), Lingshui Li Autonomous County (SE), and Sanya (S) located in the northwest, northeat, southeast and south of the island, respectively (Figure 1). Wuzhishan Nature Reserve, situated in central the Hainan Island, is a forest ecosystem nature reserve primarily driven by tourism. Changjiang Li Autonomous County, situated in the northwest of the Hainan Island, is abundant in diverse mineral resources. Haikou City and Sanya City, located in the northeast and southwest of the Hainan Island, respectively, are the two largest cities on the island, characterized by flourishing industry, commerce, and high population density. Lingshui Li Autonomous County, situated in the southeast of the Hainan Island, is predominantly reliant on tourism.

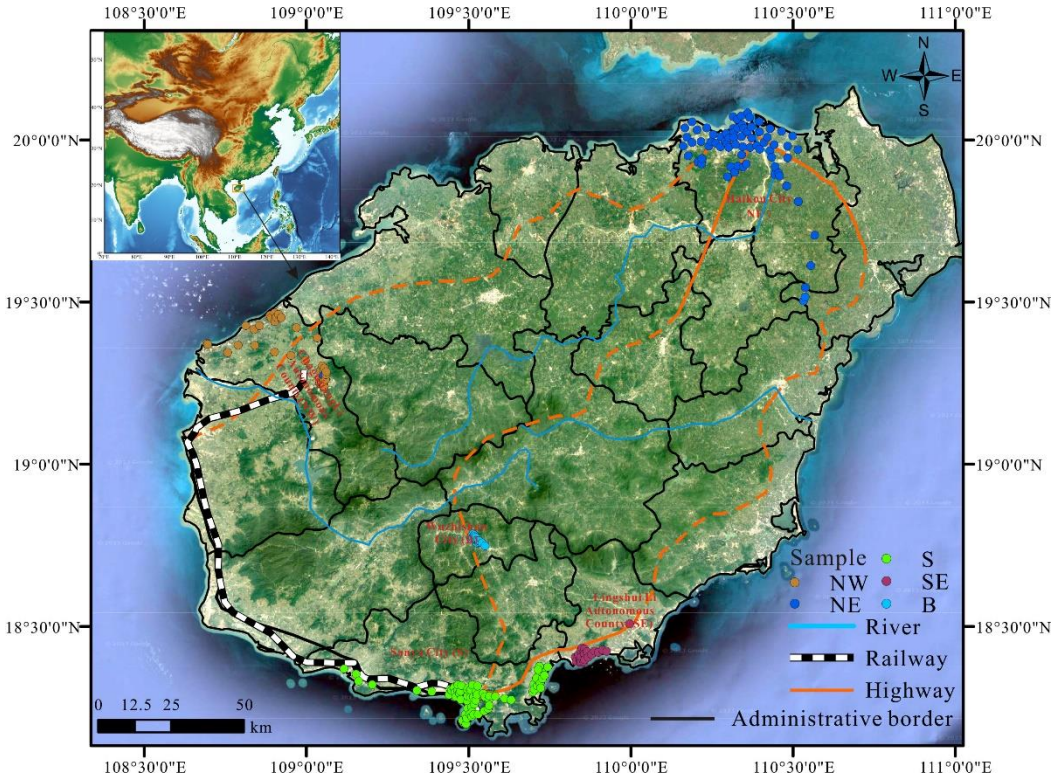

Figure 1. Location of the study area and the five sub-study areas.

 doi:10.20944/preprints202402.1449.v1

3. Materials and methods

This section may be divided by subheadings. It should provide a concise and precise description of the experimental results, their interpretation, as well as the experimental conclusions that can be drawn.

3.1. Sampling and analysis

3.1.1. Sampling and analysis of soil Hg

Samples were collected along the primary thoroughfares in the aforementioned five sub-study areas, as illustrated in Figure 1. A total of 239 samples were collected (Figure 2). The northeast (NE) and southwest (S), representing the two most developed cities, yielded the highest number of samples, nearly 80 each, accounting for approximately 33% of the total. The northwest (NW) and southeast (SE) regions followed with 41 and 25 samples, respectively, while the fewest samples were collected in the Wuzhishan Nature Reserve (B), i.e., 16 in total.

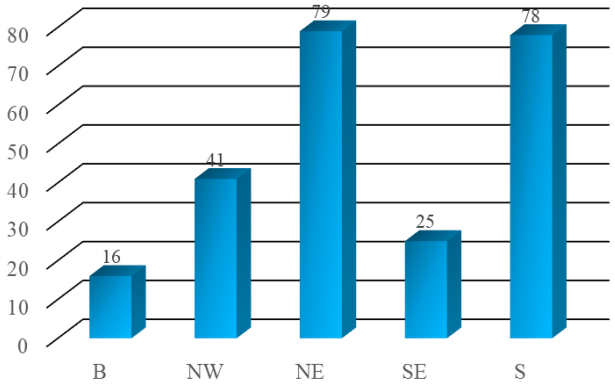

Figure 2. Number of sampling sites in each sub-study area.

3.1.2. Determination of atmospheric total Hg

At each soil sampling site, the total gaseous Hg in the atmosphere was also measured using the Mercury Analyzer RA-915M. During air sampling, all sampling points were vertically categorized into two levels, i.e., at ground surface and 100 cm above the ground. The atmospheric detection limit was set at 2 ng/m3. Each sampling point underwent 6 minutes of monitoring, meaning each layer within every point was continuously monitored for 30 seconds at a rate of one reading every 10 seconds. The monitoring cycle was repeated 6 times, resulting in 18 parallel data for each layer within every sampling point.

3.2. Methodology

3.2.1. Evaluation of soil Hg pollution

The Single Pollution Index method and the Geoaccumulation Index Method are frequently employed for assessing soil pollution levels. These methods allow for the categorization of soil Hg pollution into distinct levels (Wang et al., 2007).

The Single Pollution Index of soil Hg is calculated as

$$P_i = \frac{C_i}{S_i} \quad (1)$$

where P_i is Single Pollution Index of soil Hg; C_i is the measured concentration of Hg (mg·kg^{-1}); S_i is the evaluation standard of Hg (mg·kg^{-1}), and the average concentration of soil Hg in Wuzhishan Nature Reserve is selected as the evaluation standard here.

 doi:10.20944/preprints202402.1449.v1

In contrast to the Single Pollution Index, which only yields preliminary concentration evaluation results, the Geoaccumulation Index Method (Wang et al., 2012) not only captures the natural variation characteristics of Hg distribution, but also discerns the influence of human activities on the environment. The formula for this method is

$$I_{geo} = log_2[\frac{C_i}{k \times B_i}] \quad (2)$$

where I_{geo} is the Geoaccumulation Index; C_i is the measured concentration of Hg (mg·kg^{-1}); k is the correction index taken into consider the changes in the background value that may be caused by differences in rocks in various places. The general value is 1.5; B_i is the soil background value. In this study, the average concentration of soil Hg in Wuzhishan Nature Reserve was selected as the background value.

3.2.2. Soil Hg health risk assessment

Soil Hg primarily enters the human body via three principal routes: (i) dermal contact and subsequent ingestion, (ii) direct oral ingestion, and (iii) inhalation of airborne particulate matter. However, research suggests that Hg can also be assimilated into the body in vapor form (Chen et al., 2012). Therefore, there are four main exposure pathways in total.

Drawing upon the Chinese Environmental Site Assessment Guideline issued by Beijing Municipal Bureau of Quality and Technical Supervision (BQTS) (2009) and the environmental health risk assessment methodologies advocated by the United States Environmental Protection Agency (EPA, 1989), we present the risk models for various exposure pathways and provide the corresponding calculation formula as follows.

The route: of direct human skin contact:

$$EDI_{skin} = \frac{C \times SA \times AF \times ABS \times EF \times ED}{BW \times AT} \times 10^{-6} \quad (3)$$

In the above, *EDI* is the chronic daily exposure, mg·(kg·d)$^{-1}$; *C* is the measured concentration, mg·kg^{-1}; *SA* is the skin area that may be in contact with soil, cm^2·d^{-1}, the reference value is 5000 cm^2·d^{-1} (Du et al., 2013); *AF* is the adsorption coefficient of skin to soil, mg·cm^{-2}, the reference value is 1 mg·cm^{-2} (Vilavert et al., 2012); *ABS* is the skin respiration rate, the reference value is 0.001 (Du et al., 2013); *EF* is the exposure frequency, d·a^{-1}, the reference value is 350 d·a^{-1} (Vilavert et al., 2012); *ED* is the exposure period, a, the reference value is 25 a; *BW* is body weight, kg, the reference value is 55.9 kg (Du et al., 2013); AT is the exposure period, d, and the reference value is 365×*ED* (d) (Du et al., 2013).

The route of direct oral ingestion:

$$EDI_{oral} = \frac{C \times IFP \times EF \times ED}{BW \times AT} \times 10^{-6} \quad (4)$$

where *EDI*, *C*, *EF*, *ED*, *BW* and *AT* all refer to formula (3). *IFP* is soil intake, mg·d$^{-1,}$ the reference value is 114 mg·d^{-1} (Vilavert et al., 2012).

The route of ingestion via breathing:

$$EDI_{breath} = \frac{C \times IR \times EF \times ED}{BW \times AT \times PEF} \quad (5)$$

where *EDI*, *C*, *EF*, *ED*, *BW* and *AT* all refer to formula (3). *IR* is air intake, m^3·d^{-1}, and the reference value is 20 m^3·d^{-1} (Vilavert et al., 2012). *PEF* is the soil dust generation factor, the reference value is 1.32×10^9 (Tang et al., 2012).

The route of Hg vapor inhalation:

$$EDI_{vapor} = \frac{C \times IR \times EF \times ED}{BW \times AT \times VF} \quad (6)$$

In the above, *EDI*, *C*, *EF*, *ED*, *BW* and *AT* all refer to formula (3). *IR* refers to equation (5). VF is the evaporation coefficient, m^3·kg^{-1}, and the reference value is 32 657. 6 m^3·kg^{-1} (Chen et al., 2012).

 doi:10.20944/preprints202402.1449.v1

Health risk assessment is usually divided into carcinogenic risk assessment and non-carcinogenic risk assessment. For Hg, non-carcinogenic risk assessment is generally conducted and evaluated using the hazard quotient HQ:

$$HQ = \frac{EDI_i}{RfD_i} \quad (7)$$

In the above, EDI_i is the chronic daily exposure, mg·(kg·d)$^{-1}$; RfD_i is the reference dose for risk assessment of various pathways, mg·(kg·d)$^{-1}$; RfD_{skin} = 2.4×10^{-5} mg·(kg·d)$^{-1}$ (BQTS, 2009) ; Rf_{Doral} = 3.0×10^{-4} mg·(kg·d)$^{-1}$ (BQTS, 2009) ; $Rf_{Dbreath}$ = 1. 07×10^{-4} mg·(kg·d)$^{-1}$ (BQTS, 2009) ; Rf_{Dvapor} = 1×10^{-3} mg·(kg·d)$^{-1}$ (Chen et al., 2012).

The total non-carcinogenic risk value of Hg in different pathways is expressed as *HI*, described by

$$HI = \sum_i^n HQ_i \quad (8)$$

when *HI* or *HQ* > 1, it is considered that there is a potential non-carcinogenic risk; when *HI* or *HQ* < 1, the risk is considered to be small or negligible.

Based on the health risk assessment formulas (3) to (8), exposure calculation parameters and site data, the possible non-carcinogenic exposure risk to the local adult human body was calculated.

4. Results and discussion

4.1. Factors affecting soil Hg levels

4.1.1. Distribution characteristics of soil Hg levels

Table 1 presents the range and mean values of Hg concentrations in soil samples collected from various regions. In the Hainan Island, the Hg concentration exhibited a substantial variation from 6.04 to 1582.50 ng·g^{-1}, with a mean value of 61.51 ng·g^{-1} and a standard deviation of 147.41. The Wuzhishan Nature Reserve (B), characterized by a lower pollution potential, had an average soil Hg concentration of 32.67 ng·g^{-1}, which was adopted as the background value for soil Hg in the Hainan Island. Except for Lingshui Li Autonomous County (SE), the coastal cities including Changjiang Li Autonomous County (NW), Haikou (NE), and Sanya (S), all exhibited varying degrees of Hg contamination. Notably, Changjiang Li Autonomous County (NW) had the highest average value, approximately 4.5 times the background value, and its maximum value exceeded the background value by 48.4 times. Haikou and Sanya showed slightly elevated Hg levels compared to the background value, with average values approximately 1.6 and 1.2 times higher, respectively.

Table 1. Average and range of soil Hg concentration in the five sub-study areas (ng·g^{-1}).

Sub-study area	mean	Range	Std
B	32.67	10.70—104.67	21.61
NW	147.16	10.00—1582.50	329.43
NE	54.01	8.33—321.50	43.32
S	41.08	6.04—180.50	27.25
SE	26.96	9.43—84.00	16.52

Figure 3a-e illustrate the soil Hg concentration at each sampling site. Notably, the soil Hg concentration in Wuzhishan Nature Reserve (B) and Lingshui Li Autonomous County (SE) is generally lower compared to the other three areas (Figure 3d-e). In contrast, Changjiang Li Autonomous County (NW) exhibits the highest soil Hg concentration among the five sub-study areas, displaying a distinct pattern of high inland and low along the coast (Figure 3a). Ths phenomenon can be attributed to the presence of numerous mines inland, where ore weathering contributes to elevated soil Hg concentration. In contrast, Sanya (S) and Haikou (NE) exhibit a contrasting distribution pattern, with higher soil Hg concentration along the coast and lower levels inland (Figure 3b-c). This

 doi:10.20944/preprints202402.1449.v1

disparity may be ascribed to the more developed economy and higher traffic density in the coastal areas. Consequently, car exhaust emissions naturally settle into the soil, which can also result in increased Hg concentration in the soil.

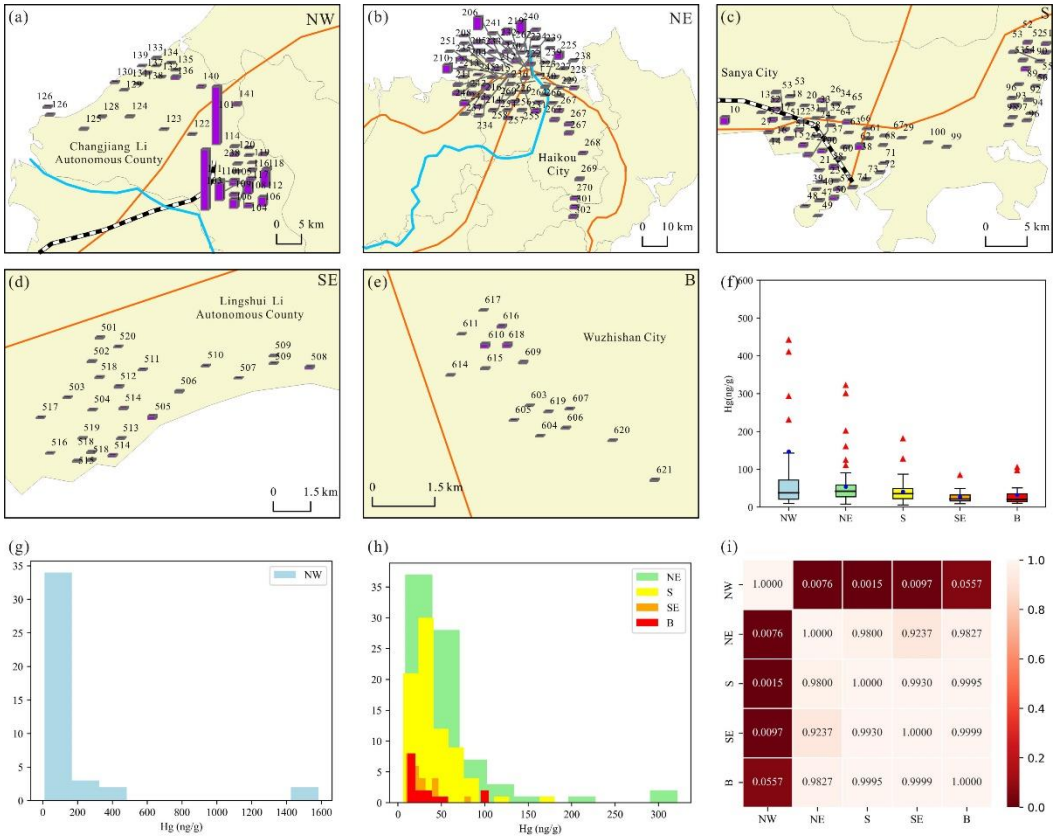

Figure 3. Characteristics of soil Hg concentration of the five sub-study areas. (a-e) distribution of soil Hg concentration, (f) Box Plot of soil Hg concentration, (g-h) Frequency Histogram of soil Hg concentration, and (i) ANOVA results of soil Hg concentration of the five sub-study areas.

4.1.2. Impact of wind direction on soil Hg

To investigate the influence of wind direction on soil Hg concentration in the Hainan Island, the five sub-study areas were selected for analysis using box plots and variance analysis. As illustrated in Figure 3f, the soil Hg concentration exhibited directional variations, with the highest concentration observed in the northwest direction. Consequently, a one-way analysis of variance (ANOVA) was conducted. The results revealed a significant difference in Hg concentration distribution among the five sub-study areas ($F = 4.63$, $P = 0.001$). Further pairwise comparisons indicated that the Hg concentration in the northwest direction was significantly distinct from that in the other directions, with P values less than 0.05. However, no significant differences were found among the Hg concentrations in the remaining three directions, as all P exceeded 0.9 and were substantially greater than 0.05 (Figure 2i).

The spatial distribution of soil Hg pollution in the Hainan Island exhibits a strong correlation with wind direction. The Hainan Island has a tropical monsoon climate characterized by predominant southeasterly winds. Consequently, the polluted atmosphere is transported northwestward, leading to the deposition of atmospheric Hg onto the corresponding soil surfaces via precipitation. The water-soluble Hg accumulated on the soil surface is subsequently leached by rain, resulting in the transportation of water-soluble Hg to the surface. This process causes runoff loss or soil infiltration (Danieal et al., 2002), resulting in significantly higher Hg concentrations in the downwind surface soil compared to the upwind surface soil. Therefore, the Hg concentration in the surface soil gradually increases from southeast to northwest. In addition to meteorological conditions (predominant wind direction), other factors that may influence soil Hg concentration include terrain

 doi:10.20944/preprints202402.1449.v1

fluctuations in the surrounding environment, physical and chemical properties of the soil, and human activities (Guo et al., 1996).

4.1.3. Relationship between soil Hg and atmospheric Hg

Figure 4 presents a comparative analysis of the atmospheric Hg concentration at the ground surface (Ground) and 100 cm above the ground (Atmosphere). The majority of sampling points (95%) exhibit significant variations in Hg concentrations between the two levels (Figure 4a). Notably, 101 points (42%) show lower atmospheric Hg concentrations at the ground surface compared to 100 cm above the ground (Figure 4b). This phenomenon can be attributed to secondary dust, as these sampling points are situated on streets with relatively heavy traffic flow. Consequently, the prevalence of secondary dust leads to elevated atmospheric Hg concentration at 100 cm compared to the ground surface. Furthermore, the results of Pearson Correlation Analysis reveal statistically significant positive correlations ($P < 0.05$, $R^2 > 0.7$) between the Hg concentrations at the ground surface and 100 cm above the ground in all five sub-study areas (Table 2).

Table 2. Pearson correlation coefficient of atmospheric Hg concentration at the ground surface and 100 cm above the ground.

		All	NW	NE	S	SE	B
All	R^2	0.613	0.495	0.488	0.827	0.173	0.797
	P	$6.6770 \cdot 10^{-26}$	0.0010	5.1767	$1.0334 \cdot 10^{-20}$	0.4078	0.0004
A>G	R^2	0.830	0.829	0.740	0.931	0.788	0.802
	P	$7.3478 \cdot 10^{-27}$	$3.9269 \cdot 10^{-5}$	$2.4565 \cdot 10^{-5}$	$1.0557 \cdot 10^{-5}$	$0.0023 \cdot 10^{-5}$	$0.1982 \cdot 10^{-5}$
A<G	R^2	0.789	0.786	0.752	0.928	0.516	0.932
	P	$1.3148 \cdot 10^{-27}$	$2.3977 \cdot 10^{-5}$	$5.0836 \cdot 10^{-8}$	$2.3671 \cdot 10^{-18}$	0.0708	$2.9877 \cdot 10^{-5}$

Concurrently, 125 points (53%) exhibited higher atmospheric Hg concentrations at the ground surface compared to 100 cm above the ground. This phenomenon is associated with the natural deposition of dust in the atmosphere. The correlation analysis revealed a significant positive correlation between the atmospheric and soil Hg concentrations ($R^2 = 0.789$, $P = 1.314 \times 10^{-27}$) (Table 3). Previous research by Wang et al. (1998) suggested a strong positive correlation between atmospheric and soil Hg concentrations, indicating that higher atmospheric Hg concentration correspond to elevated soil Hg concentration. However, our correlation analysis results indicate an absence of significant correlation between atmospheric and soil Hg concentrations ($P = 0.95 > 0.05$). Considering the findings from the previous section, the Hainan Island experiences a pronounced monsoon, which facilitates the transport of atmospheric Hg pollutants. This transport process influences the natural deposition of Hg into the soil, thereby weakening the correlation between atmospheric and soil Hg concentrations.

 doi:10.20944/preprints202402.1449.v1

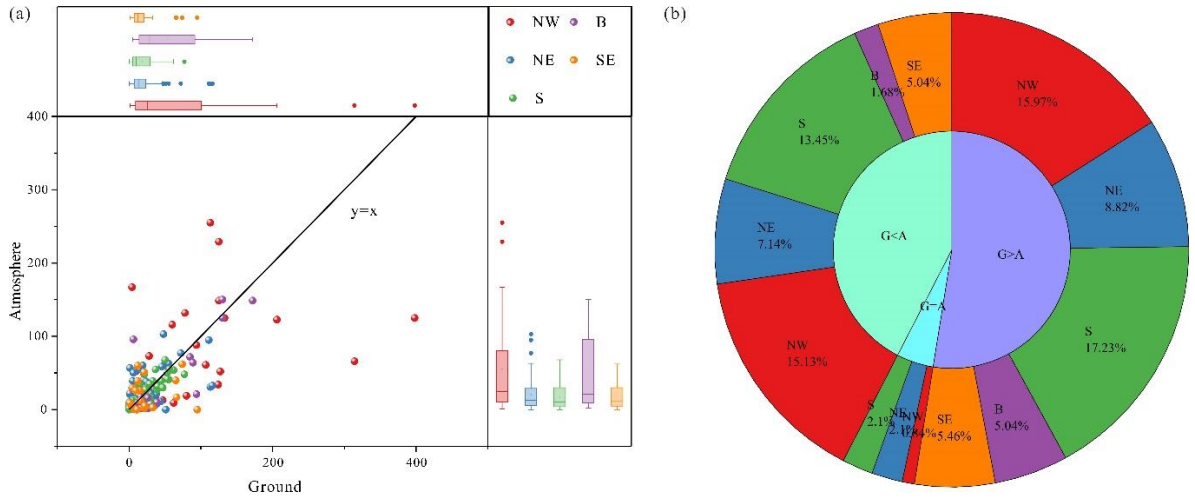

Figure 4. (a) Comparison of atmospheric Hg concentration at the ground surface (G) and at 100 cm above the ground (A) (ng·m^{-3}), and (b) the proportion of each area.

Table 3. Pearson correlation coefficient of atmospheric Hg at the ground surface and soil Hg concentrations.

		All	NW	NE	S	SE	B
All	R^2	-0.063	-0.134	-0.049	-0.102	-0.069	-0.237
	P	0.3348	0.4092	0.6705	0.3755	0.7420	0.3941
A>G	R^2	-0.061	-0.211	-0.115	0.025	-0.103	-0.424
	P	0.5455	0.4152	0.5031	0.8923	0.7489	0.5756
A<G	R^2	-0.006	-0.165	-0.028	-0.152	-0.158	-0.041
	P	0.9512	0.4737	0.8664	0.3413	0.6070	0.8997

4.2. Hg pollution assessment

4.2.1. Soil Hg Pollution Assessment

Table S1 presents the calculated results for the Single Pollution Index (P_i) and Geoaccumulation Index (I_{geo}). The corresponding column graphs are provided in Figure 5.

 doi:10.20944/preprints202402.1449.v1

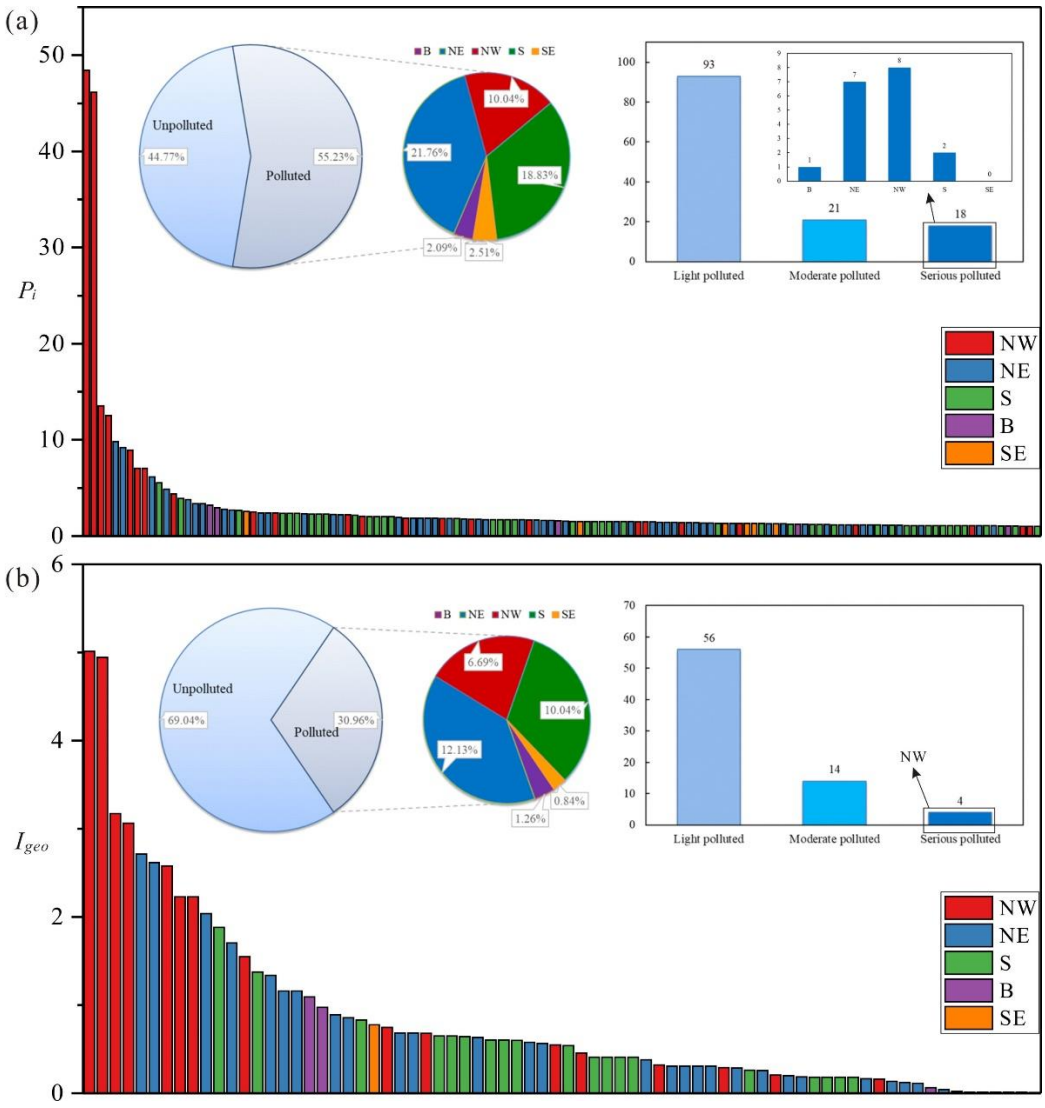

Figure 5. Sigle Pollution Index (a) and Geoaccumulation Index (b) of Soil Hg, the Hainan Island.

Based on the evaluation criteria of the Single Pollution Index (Figure 5a), 55.23% of the sampling points were found to be contaminated (P_i > 1). Notably, the highest proportions of contaminated points were observed in the NE (21.76%) and S (18.83%) regions, followed by NW (10.04%), B (2.09%), and SE (2.51%). A closer examination of the P_i values revealed that 18 sampling points exhibited severe pollution (P_i > 3), with NW and NE regions accounting for the majority (8 and 7 points, respectively). Additionally, 2 points in the S region and 1 point in the B region were classified as severely polluted. Among these, points 111 and 101 in the NW area exhibited the highest pollution levels, with Pi values of 48.4 and 46.1, respectively, indicating extremely severe pollution. Furthermore, 21 sampling points (8.8% of the total) were moderately polluted (2 < P_i < 3), while a substantial number of points (93, accounting for 38.9% of the total) exhibited mild pollution (1 < P_i < 2).

Considering the cumulative pollution index as the evaluation criterion (Figure 5b), approximately 30.96% of the sampling points were found to be polluted (I_{geo} > 0). Similar to the P_i-based analysis, NE and S regions had the highest proportions of polluted points (12.13% and 10.04%, respectively), followed by NW (6.69%), B (1.26%), and SE (0.84%). An analysis of the I_{geo} values indicated that only 4 sampling points were severely polluted (I_{geo} > 3), all of which were located in the NW region. Fourteen sampling points (5.8% of the total) were moderately polluted (1 < I_{geo} < 3), while a larger number of points (56, accounting for 23.4% of the total) were mildly polluted (0 < I_{geo} < 1).

 doi:10.20944/preprints202402.1449.v1

4.2.2. Soil Hg Health Risk Assessment

Appendix A presents the calculated *HI* for the soil. The *HI* for all samples across the five sub-study areas ranges between 0.0001 to 0.0334, which is significantly lower than 1, indicating that soil Hg pollution within the study area does not pose a significant health risk to humans.

The average *HI* for the five sub-study areas, arranged in descending order, are as NW > NE > S > B > SE (Figure 6). This trend is consistent with the analysis results obtained from the pollution index. Changjiang Li Autonomous County (NW), situated on the northwest coast of the island and in the downwind direction, is home to numerous mines. Consequently, this region exhibits higher soil Hg concentration, more severe pollution, and a higher health risk compared to the other areas. Haikou City (NE) and Sanya City (S), the two largest cities on the Hainan Island, are characterized by developed economies and thriving industries and commerce. As a result, these regions show higher levels of soil Hg pollution and higher health risks compared to the Wuzhishan Nature Reserve (B) and Lingshui Li Autonomous County (SE). The Wuzhishan Nature Reserve (B) suffers fewer human activities, and exhibits relatively lighter Hg pollution and lower health risks, while Lingshui Li Autonomous County (SE), located on the southeast coast and in the wind direction of the monsoon, has the lowest levels of pollution and health risks. Therefore, the health risk posed by atmospheric and soil Hg pollution is mostly from mining and traffic, and impacted by the transportation of wind.

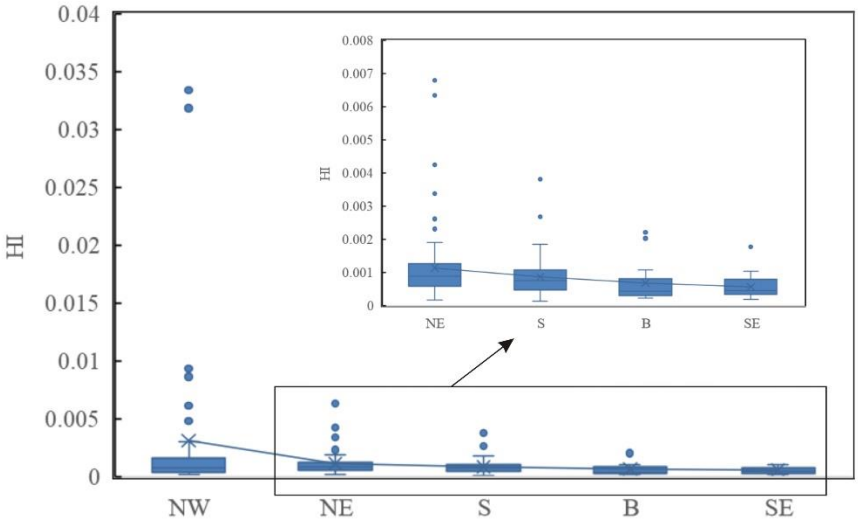

Figure 6. Box Plot of Health Risk Index (HI) in each sub-study area, the Hainan Island.

5. Conclusion

The soil Hg level in the Hainan Island spans a range of 6.04 to 1582.50 $ng \cdot g^{-1}$, averaged 61.51 $ng \cdot g^{-1}$. Significant regional variation is observed, with Changjiang Li Autonomous County abundance in mineral resources showing the highest concentration, followed by the economically developed cities Haikou and Sanya, while the Wuzhishan Nature Reserve and Lingshui Li Autonomous County exhibit the lowest concentrations. Wind direction notably influences soil Hg content, with higher levels observed downwind (northwest) compared to upwind (southeast). A strong positive correlation is found of between the atmospheric Hg concentrations at ground surface and 100 cm above the ground, whereas a weak correlation exists between the contents of soil Hg and atmospheric Hg at ground surface.

Based on the Single Pollution Index method and the Geoaccumulation Index method, nearly half of the sampling points indicated Hg pollution. However, the current pollution level is not deemed sufficient to pose a non-carcinogenic risk to human health. However, continuous monitoring of the soil Hg content and health risk assessment is necessary as the fast development of traffic, mining and industrialization.

Supplementary Materials: The following supporting information can be downloaded at: Table S1: Data of atmospheric and soil Hg and parameters used in risk assessment.

Author Contributions: Conceptualization, Y.S. and C.Y.; methodology, Y.S.; software, Y.S.; validation, C.Y.; formal analysis, Y.S.; investigation, Y.S.; resources, Y.S. and C.Y.; data curation, Y.S.; writing—original draft preparation, Y.S.; writing—review and editing, C.Y.; visualization, Y.S.; supervision, C.Y.; project administration, C.Y.; funding acquisition, C.Y. All authors have read and agreed to the published version of the manuscript.

Funding: Please add: This research was funded by the Education Department of Hainan Province (HnjgY2022-12) and the National Natural Science Foundation of China (32260127).

Institutional Review Board Statement: Not applicable.

Informed Consent Statement: Not applicable.

Data Availability Statement: Data are contained within the article and supplementary materials.

Acknowledgments: We thank Prof. Zhang gang at School of Environment, Northeast Normal University for the help in Hg measurement and insightful discussion.

Conflicts of Interest: The authors declare no conflicts of interest.

References

1. Meriga, B.; Krishna Reddy, B.; Rajender Rao, K.; Ananda Reddy, L.; Kavi Kishor, P.B. Aluminum-induced production of oxygen radicals, lipid peroxidation and DNA damage in seedlings of rice (Oryza sativa). *J. Plant Physiol.* **2004**, *161*, 63–68. https://doi.org/10.1078/0176-1617-01156.
2. Futsaeter, G.; Wilson, S. The UNEP global mercury assessment: sources, emissions and transport. In Proceedings of the 16th International Conference on Heavy Metals in the Environment, Rome, Italy 23 - 27 September 2012; pp.973–974.
3. Carocci, A.; Rovito, N.; Sinicropi, M.S.; Genchi, G. Mercury Toxicity and Neurodegenerative Effects. In: Whitacre, D. (eds.) Reviews of environmental contamination and toxicology. *Rev. Environ. Contam. & Toxicol.* **2014**, *229*, 1–18. https://doi.org/10.1007/978-3-319-03777-6_1.
4. Cheng, P.L. The sociological research on "Minamata Disease" in Japan (in Chinese with English abstract). *J. Hohai Univ. (Philos. & Social Sci.)*, **2008**, *10*, 30–33.
5. Taylor, J. Mercury reduction efforts in Michigan. *Fuel Process. Technol.* **2000**, *60*, 69–77. https://doi.org/10.1016/S0378-3820(99)00077-6.
6. Martin, L.; Pekka, N.; Sirkka-Liisa, N. Uptake of mercury by terrestrial plants-observations in Fin-land and Slovenia in the years 1979~1981. *Mater. & Geoenviron*. **2004**, *51*, 1181~1184.
7. Hu, Y. Reviews of Mercury pollution distribution status research at home and abroad (in Chinese with English abstract). *Environ. Prot. Sci.* **2008**, *34*, 38–41.
8. Kang, H.; Liu, X.; Guo, J.; Xu, G.; Wu, G.; Zeng, X.; Wang, B.; Kang, S. Increased Mercury Pollution Revealed by Tree Rings from the China's Tianshan Mountains. *Sci. Bull.* **2018**, *63*, 1328–1331. https://doi.org/10.1016/j.scib.2018.09.010.
9. Yin, W.; Lu, Y.; Li, L.; Chen, C.; Zhang, C.; Dong, F. Distribution characteristics and pollution assessment of mercury in urban soils of Guangzhou (in Chinese with English abstract). *Chin. J. Soil Sci.* **2009**, *40*, 1185–1188.
10. Xu, J.; Bravo, A.G.; Lagerkvist, A.; Bertilsson, S.; Sjöblom, R.; Kumpiene, J. Sources and remediation techniques for mercury contaminated soil. *Environ.Int.* **2015**, *74*, 42–53. https://doi.org/10.1016/j.envint.2014.09.007.
11. Lindberg, S.; Bullock, R.; Ebinghaus, R.; Engstrom, D.; Feng, X.; Fitzgerald, W.; Pirrone, N.; Prestbo, E.; Seigneur, C. A synthesis of progress and uncertainties in attributing the sources of mercury in deposition. *Ambio*. **2007**, *36*, 19–33. https://doi.org/10.1579/0044-7447(2007)36[19:ASOPAU]2.0.CO;2.
12. Fang, F.; Wang, Q.; Li, J. Urban environmental mercury in Changchun, a metropolitan city in Northeastern China: source, cycle and fate. *Sci. Total Environ.* **2004**, *330*, 159-170. https://doi.org/10.1016/j.scitotenv.2004.04.006.
13. Rodrigues, S.; Pereira, M.E.; Duarte, A.C.; Ajmone-Marsan, F.; Davidson, C.M.; Grčman, H.; Hossack, I.; Hursthouse, A.S.; Ljung, K.; Martini, C.; Otabbong, E.; Reinoso, R.; Ruiz-Cortés, E.; Urquhart, G.J.; Vrščaj, B. Mercury in urban soils: a comparison of local spatial variability in six european cities. *Sci. Total Environ.* **2006**, *368*, 926–936. https://doi.org/10.1016/j.scitotenv.2006.04.008.
14. Zhang, L.; Wang, M. Environmental mercury contamination in China: sources and impacts. *Environ. Int.* **2007**, *33*, 108–121. https://doi.org/10.1016/j.envint.2006.06.022.

15. Friedli, H.R.; Radke, L.F.; Lu, J.Y.; Banic, C.M.; Leaitch, W.R.; MacPherson, J.I. Mercury emissions from burning of biomass from temperate north american forests: laboratory and airborne measurements. *Atmos. Environ.* **2003**, *37*, 253–267. https://doi.org/10.1016/S1352-2310(02)00819-1.
16. UNEP. Global mercury assessment 2013: sources, emissions, releases and environmental transport. UNEP Chemicals Branch: Geneva, Switzerland, 2013.
17. Chen, B.; Li, J.S.; Chen, G.Q.; Wei, W.D.; Yang, Q.; Yao, M.T.; Shao, J.A.; Zhou, M.; Xia, X.H.; Dong, K.Q.; Xia, H.P.; Chen, H.P. China's energy-related mercury emissions: characteristics, impact of trade and mitigation policies. *J. Cleaner Prod.* **2017**, *141*, 1259–1266. http://dx.doi.org/10.1016/j.jclepro.2016.09.200.
18. Zhao, S.; Pudasainee, D.; Duan, Y.; Gupta, R.; Liu, M.; Lu, J. A review on mercury in coal combustion process: concentration and occurrence forms in coal, transformation, sampling methods, emission and control technologies. *Prog. Energy Combust. Sci.* **2019**, *73*, 26–64. https://doi.org/10.1016/j.pecs.2019.02.001.
19. Liao, Z.P.; Chen, Y.C.; Yang, X.C.; Wei, S.Q. Assessment of potential ecological hazard of heavy metals in urban soils in Chongqing City (in Chinese with English abstract). *J. Southwest Agricul. Univ.* **2006**, *2*, 227–230.
20. Huang, S.; Wu, X.; Yan, C. Heavy metal concentrations and their spatial distribution in urban soils of Nanjing (in Chinese with English abstract). *Urban Environ. & Urban Ecol.* **2007**, *20*, 1–4.
21. Wang, X.S.; Qin, Y.; Sang, S.X. Accumulation and sources of heavy metals in urban topsoils: a case study from the city of Xuzhou, China. *Environ.Geol.* **2005**, *48*, 101–107. https://doi.org/10.1007/s00254-005-1270-x.
22. Qian, J.; Zhang, L.; Liu, H.; Ye, J. Soil mercury distribution and pollution in urban and suburbs of Guilin (in Chinese with English abstract). *Geochim.* **2000**, *1*, 94–99.
23. Zhang, X.; Luo, K.; Sun, X.; Sun, X.; Tan, J.; Lu, Y. Mercury in the topsoil and dust of Beijing City. *Sci. Total Environ.* **2006**, *368*, 713-722. https://doi.org/10.1016/j.scitotenv.2006.01.037.
24. Guo, C.; Wang, Y.; Ren, Y.; Shi, J. The distribution characteristics of Hg-element concentration in the surface soil in Taiyuan (in Chinese with English abstract). *J. Shanxi Univ. (Nat. Sci. Ed.)*, **1996**, *19*, 339–344.
25. Zhang, X. Research on the environmental background values of soils in Xizang (in Chinese with English abstract). *Sci. Geogr. Sin.* **1994**, *14*, 49–54.
26. Hu, H. The Investigation of The Heavy Metal Pollution in The Aningqu District (in Chinese with English abstract). *Arid Environ. Monit.* **2023**, *17*, 117–122.
27. Manta, D.S.; Angelone. M.; Bellanca, A.; Neri, R.; Sprovieri, M. Heavy metals in urban soils:a case study from the city of Palermo (Sicily), Italy. *Sci. Total Environ.* 2002, 300, 229–243. https://doi.org/10.1016/S0048-9697(02)00273-5.
28. Kot, F.S.; Matyushkina, L.A. Distribution of mercury in chemical fractions of contaminated urban soils of Middle Amur, Russia. *J. Environ. Monit.* **2002**, *4*, 803-808. https://doi.org/10.1039/B203414J.
29. Zhou, Y.; Ma, S.; Zhu, W.; Shi, Q.; Jiang, H.; Lu, R.; Wu, W. Revealing varying relationships between wastewater mercury emissions and economic growth in Chinese cities. *Environ. Pollut.* **2024**, *341*, 1–10. https://doi.org/10.1016/j.envpol.2023.122944.
30. Guo, S.; Wang, Y. Spatial-temporal changes of land-use mercury emissions in China, *Ecol. Indic.* **2023**, *146*, 1-10. https://doi.org/10.1016/j.ecolind.2022.109430.
31. Wang, L.; Lu, X.; Wang, L.; Jia, X.; Wang, F. Evaluation of Hg soil around the Baoji coal-fired power plant (in Chinese with English abstract). *China J. Soil Sci.* **2007**, *38*, 622–624.
32. Wang, L.; Lu, X.; Jing, Q.; Ren, C.; Chen, C.; Li, X.; Luo, D. Heavy metals pollution in soil around the lead-zinc smelting plant in Changqing Town of Baoji City, China (in Chinese with English abstract). *J. Agro-Environ. Sci.* **2012**, *31*, 325-330.
33. Chen, P.; Qiu, H.Y.; Guo, Y.N.; Wang, L.Y. Heavy metal contamination and health risk assessment in the zinc mine set area of Youxi, China (in Chinese with English abstract). *J. Xiamen Univ. (Nat. Sci.)*, **2012**, *51*, 245-251.
34. BQTS (Beijing Municipal Bureau of Quality and Technical Supervision). Environmental site assessment guideline (DB11 T 656-2009, in Chinese), 2009, pp. 1-41.
35. EPA. Risk Assessment Guidance for Superfund Volume I: Human Health Evaluation Manual (Part A). 1989, pp. 1-291.
36. Du, Y.; Gao, B.; Zhou, H.; Ju, X.; Hao, H.; Yin, S. Health risk assessment of heavy metals in road dusts in urban parks of Beijing, China. *Procedia Environ. Sci.* **2013**, *18*, 299-309. https://doi.org/10.1016/j.proenv.2013.04.039.
37. Vilavert, L.; Nadal, M.; Schuhmacher, M.; Domingo, J.L. Concentrations of metals in soils in the neighborhood of a hazardous waste incinerator: assessment of the temporal trends. *Biol. Trace Elem. Res.* **2012**, *149*, 435–442. https://doi.org/10.1007/s12011-012-9441-6.
38. Tang, R.; Ma, K.; Zhang, Y.; Mao, Q. Health risk assessment of heavy metals of street dust in Beijing (in Chinese with English abstract). *Acta Sci. Circumst.* **2012**, *32*, 2006-2015.
39. Danieal, S.M.; Massimo, A.; Adriana, B.; Rodolfo, N.; Mario, S.H. Metals in urban soil: a case study from the City of Palermo (Sicily), Italy. the *Sci. Total Environ.* **2002**. *300*, 229-243. https://doi.org/10.1016/S0048-9697(02)00273-5.

 doi:10.20944/preprints202402.1449.v1

40. Wang, D.; Shi, X.; Yang, X. Transformation of atmospheric mercury in soil and its influence on the accumulation of mercury in soil (in Chinese with English abstract). *Chongqing Environ. Sci.* **1998**, 20, 22-25.